

Final Technical Report

COVER PAGE

Report Submitted to: DOE EERE – Water Power Technologies Office

Recipient: Florida Atlantic University, DUNS Number: 004147534

Award Number: DE-EE0006787

Project Title: Multi-static Serial LiDAR for Surveillance and Identification of Marine Life at MHK Installations

Project Period: October 1, 2014 – March 31, 2017

Principal Investigator: Gabriel M. Alsenas, SNMREC Director, galsenas@fau.edu, 561-297-0954

Report Submitted by: Gabriel M. Alsenas, SNMREC Director, galsenas@fau.edu, 561-297-0954

Date of Report: June 30, 2017

Covering Period: October 1, 2014 – March 31, 2017

Report Frequency: Project End

Award Recipient: Florida Atlantic University (FAU)

Working Partners: None

Cost Sharing Partners: None

DOE Project Team:

DOE HQ Program Manager – Alejandro Moreno
DOE Field Contract Officer – Pamela Brodie
DOE Field Grants Management Specialist – Jane Sanders
DOE Field Project Officer – Corey Vezina
DOE/AST Project Monitor – Nicholas Massey
DOE/AST Technical Monitors – Samantha Eaves and Dana McCoskey

Signature of Submitting Official:

A handwritten signature in blue ink, appearing to read "G. M. Alsenas".

This report is based upon work supported by the U. S. Department of Energy under
Award No. DE-EE0006787.

Disclaimer: Any findings, opinions, and conclusions or recommendations expressed in this report are those of the author(s) and do not necessarily reflect the views of the Department of Energy.

Proprietary Data Notice: If there is any patentable material or protected data in the report, the recipient, consistent with the data protection provisions of the award, has marked the appropriate block in Section K of the DOE F 241.3, clearly specified it here, and identified them on appropriate pages of the report. Other than patentable material or protected data, reports must not contain any proprietary data (limited rights data), classified information, information subject to export control classification, or other information not subject to release. Protected data is specific technical data, first produced in the performance of the award, which is protected from public release for a period of time by the terms of the award agreement. Reports delivered without such notice may be deemed to have been furnished with unlimited rights, and the U.S. Government assumes no liability for the disclosure, reproduction or use of such reports.

Executive Summary

This project developed and tested an optical monitoring system prototype that will be suitable for marine and hydrokinetic (MHK) full project lifecycle observation (baseline, commissioning, and decommissioning), with automated real-time classification of marine animals. This system can be deployed to collect pre-installation baseline species observations at a proposed deployment site with minimal post-processing overhead. To satisfy deployed MHK project species of concern (e.g. Endangered Species Act-listed) monitoring requirements, the system provides automated tracking and notification of the presence of managed animals within established perimeters of MHK equipment and provides high resolution imagery of their behavior through a wide range of conditions. During a project's decommissioning stage, the system can remain installed to provide resource managers with post-installation data.

Our technology, known as an Unobtrusive Multi-static Serial LiDAR Imager (UMSLI), is a technology transfer of underwater distributed LiDAR imaging technology that preserves the advantages of traditional optical and acoustic solutions while overcoming associated disadvantages for MHK environmental monitoring applications. This new approach is a purposefully-designed, reconfigurable adaptation of an existing technology that can be easily mounted on or around different classes of MHK equipment. The system uses low average power red (638nm) laser illumination to be invisible and eye-safe to marine animals and is compact and cost effective. The equipment is designed for long term, maintenance-free operations, to inherently generate a sparse primary dataset that only includes detected anomalies (animal presence information), and to allow robust real-time automated animal classification/identification with a low data bandwidth requirement. Advantages of the technology over others currently being used or being considered for MHK monitoring include:

- Unlike a conventional camera, the depth of field is near-infinite and limited by attenuation (approximately 5-8 m) rather than focal properties of a lens;
- Operation in an adaptive mode which can project a sparse grid of pulses with higher peak power for longer range detection (>10 meters) and track animals within a zone of interest with high resolution imagery for identification of marine life at closer range (<5m);
- System detection limit and Signal-to-Noise-Ratio is superior to a camera, due to rejection of both backscattering component and ambient solar background;
- Multiple wide-angle pulsed laser illuminators and bucket detectors can be flexibly configured to cover a 4pi steradian (i.e. omnidirectional) scene volume, while also retrieving 3D features of animal targets from timing information;
- Process and classification framework centered around a novel active learning and incremental classification classifier that enables accurate identification of a variety of marine animals automatically;
- A two-tiered monitoring architecture and invisible watermarking-based data archiving and retrieving approach ensures significant data reduction while preserving high fidelity monitoring.
- A methodology to train and optimize the classifier for target species of concern to optimize site monitoring effectiveness

This technological innovation addresses a high priority regulatory requirement to observe marine life interaction near MHK projects. Our solution improves resource manager confidence that any interactions between marine animals and equipment are observed in a cost-effective and automated manner. Without EERE funding, this novel application of multi-static LiDAR would not have been available to the MHK community for environmental monitoring.

Table of Contents

Executive Summary	3
Table of Figures	5
1.0 Project Objective:	6
2.0 Technical Scope Summary:	6
3.0 Project Outcomes and Results	13
3.1 UMSLI System Design, Specification, and Assembly	13
3.1.1 Performance Metric Selection	13
3.1.2 Preliminary Design	19
3.1.3 Final Design	20
3.2 Prototype Demonstration in Controlled Environment	28
3.2.1 Controlled Testing Environment	28
3.2.2 System Demonstration and Performance	28
3.3 Prototype Demonstration in Operational Environment	33
3.3.1 Operational Environment Testing Approach	33
3.3.2 Results	34
4.0 Products/Deliverables	38
4.1 Publications	38
4.2 Theses & Dissertations	38
4.3 Invited Presentations and Conferences:	38
4.4 Patents:	38
5.0 Partner Organizations	38
6.0 Recommendations and Conclusions	39

Table of Figures

Figure 1 - Left: Laser Line Scan image of entire drum cycle. Right: cropped section of BoW technical target showing target dimensions and image quality analysis regions. The target reflectance was measured in air using a laser and fiber-coupled spectrometer pair.....	14
Figure 2 - Example processed image performance at different turbidities (SSIM metrics).....	16
Figure 3 - Illustration of one single datum which consists of the objects at two different poses.	18
Figure 4 - UMSLI overall processing framework.....	19
Figure 5 - Final UMSLI system diagram.....	20
Figure 6 - Rendering showing a constellation of strategically positioned scanned laser transmitters illuminating a complete volume around an MHK device with a greater than 10 meter detection range and 5 meter identification range.....	21
Figure 7 - Fully assembled UMSLI receiver (right) and transmitter (left).....	21
Figure 8 - Process for generating a simulation dataset for the classifier.....	22
Figure 9 - Comparison of registration performance of proposed SC and MCC-based shape matching technique against some existing methods.	24
Figure 10 - Template matching classification described in a flow chart.	24
Figure 11 - Illustration of shape registration and similarity cost evaluation. The MCC affine registration results are good for both SC (upper right) and IDSC (lower left) descriptors. Yet neither descriptor actually gives perfect correspondences.....	25
Figure 12 - Chosen template shapes. From top to bottom: amberjack, barracuda, and turtle.....	25
Figure 13 – Watermark embedding process.	27
Figure 14 - Content retrieval process.....	27
Figure 15 - FAU HBOI optical testing tank and laboratory.....	28
Figure 16 - Artificial realistic aquatic life targets used during controlled environment testing.....	28
Figure 17 - USAF technical target used to resolve smallest bar and thus resolution.	29
Figure 18 - Similarity measures of test tank data.	31
Figure 19 - Detection performance.....	33
Figure 20 - UMSLI baseline prototype being transported to test site (top left) and deployed (right) in SE Florida during March 2017 field testing. Shown in bottom left are the dimensions (in inches) of the current package.....	34
Figure 21 - An image capture sequence taken at 1 frame per second from one of six UMSLI channels.....	34
Figure 22 - Raw image captures from field tests of juvenile barracuda. Gate time changes shown on the right.	35
Figure 23 - Raw image captures from field tests of grouper. Gate time changes shown on the right.	36

1.0 Project Objective:

The objective of the project was to design and construct a field-deployable Unobtrusive Multi-static Serial LiDAR Imager (UMSLI) system prototype and demonstrate the feasibility of the system to produce an omnidirectional, volumetric video stream in surveillance of the surroundings of a marine hydrokinetic (MHK) device with processing and real-time detection methods which significantly reduce an operators' monitoring overhead. The final system is extensible to a variety of MHK installations, including wave, tidal, and ocean current projects. In addition, the UMSLI system is adaptable for small, medium, or full scale device scales in any coastal environment being proposed for MHK development.

2.0 Technical Scope Summary:

To achieve project objectives during a 30 month performance period, budget period 1 (months 1-18) involved preliminary design and assembly of the hardware sub-systems as well as the design of an overall processing framework, including an active learning classifier. During budget period 2 (months 19-30), the team performed hardware testing and validation, finalized software implementation, and performed field verification of a complete system prototype.

The project was divided into five tasks: (1) UMSLI system design, specification, assembly, (2) Prototype demonstration in controlled environment, (3) Prototype demonstration in operational environment, (4) Automated video classification software development and testing, and (5) Project management.

The project's approved work plan that was successfully implemented is included for reference:

Work Plan:

BUDGET PERIOD 1: Month 1 – Month 18

Task 1: UMSLI System Design, Specification and Assembly (M1-M12)

Task Summary: The overall objective of this task was to design and construct a prototype multistatic laser imager which meets the operational requirements and end-user needs for MHK monitoring and surveillance applications.

Subtask 1.1: Establish Quantitative Performance Metrics

Subtask Summary: Following the project Kick-off meeting, the project team established the various quantitative metrics that were used throughout the project to assess the performance of the both the LiDAR demonstration and the classification software. The team has extensive experience in developing and applying image quality metrics, such as contrast, spatial resolution, contrast signal noise ratio (CSNR) and also structural similarity indices (SSIM) for underwater LiDAR imager systems.¹ The quantitative performance metrics that were to be used to assess the classifier algorithm were expected to make use of receiver operating characteristic (ROC) curve approach (e.g. false negative rate vs. object distance, false positive rate vs. object distance) under a realistic range of several pre-defined water turbidities.²

¹ Dalgleish, F.R., Vuorenkoski, A.K., Nootz, G.A., Ouyang, B. and Caimi, F.M., (2013) 'Experimental Study into the Performance Impact of Environmental Noise on Undersea Pulsed Laser Serial Imagers', *Journal of Underwater Acoustics (USN)*, Volume 61, Issue 4. Ouyang B., Dalgleish F. R., Caimi F. M., Giddings T. E., Shirron J. J., Vuorenkoski A. K., Nootz G., Britton W. and Ramos B., (2013) 'Compressive Sensing Underwater Laser Serial Imaging Systems', *Journal of Electronic Imaging, special edition on Compressive Sensing*, Vol. 22, Issue 2.

Dalgleish, F. R., Caimi, F. M., Britton W. B. and Andren C. F., (2009). "Improved LLS Imaging Performance in Scattering-dominant Waters," *Proc. of SPIE*, Vol. 7317.

² A similar application of the ROC curve metric was discussed in [Principe, "Information Theoretic Learning: Renyi's Entropy and Kernel Perspectives", page 404]

Subtask 1.2: Functional baseline and requirements analysis (M1-M2)

Subtask Summary: The team analyzed and reviewed available resources and component technologies in the context of the functional and quantitative performance requirements to develop a system-level architecture of the UMSLI functionality.

Subtask Details: Detailed analyses of operational and environmental requirements such as the quantitative performance metrics used throughout the project, site-specific parameters for target field demonstration, interface requirements, power availability, deployment and installation constraints, reliability, safety and maintainability requirements, as well as structural requirements were completed. Analyses involved application-specific consideration of key subsystem functional requirements; for example, the wavelength of the transmitter was determined by compromising between the UMSLI range (limited by attenuation) and the visual physiology of the target species. While the optimal wavelength for extended range is between 400 nm and 700 nm, the chosen wavelength was long enough to make sure the light source invisible to target species and therefore ensured the system does not alter the behavior of the animals. A review of literature for both marine mammals and marine turtles determined that the use of illumination above 625nm is beyond the spectral sensitivity range for such target species.

Milestone 1.2.1: Preliminary Design Review (PDR) (M2)

Subtask 1.3: System/subsystem design and specification (M2-M5)

Subtask Summary: System/subsystem specifications (component selection, drawings, assemblies, analytical performance predictions, control and data acquisition hardware and software) were developed. Selection of commercial off-the-shelf (COTS) modules and components were made where possible. These include system performance, power budget analysis, heat budget analysis, assessment of component and subsystem manufacturing readiness level (MRL), and system cost analysis. The outcome of the detailed design task was the component-level system design, which also defined the major system parameters, such as the number of transmitter/receiver modules, field of view, scan angle and frequency, operational modes (high-resolution/low resolution, coverage and expected range).

Milestone 1.3.1: Critical design review (M5)

Subtask 1.4: Subsystem and component procurement (M6-M7)

Subtask Summary: Following the critical design review meeting, the various components and modules were ordered.

Milestone 1.4.1: All UMSLI components arrived at Florida Atlantic University

Subtask 1.5: High-fidelity laboratory integration of components/breadboard (M7-M8)

Subtask Summary: Components were assembled on a breadboard into a functional system. The major tasks were to develop FPGA control software to interface with multiple illuminator modules, control triggering of specific laser illuminators, and triggering and timing of data acquisition from specific detectors. All subsystems and components were thoroughly tested before system integration.

Milestone 1.5.1: UMSLI breadboard system assembled and control software implemented

Subtask 1.6: Component and breadboard validation in a relevant environment (M9-M10)

Subtask Summary: Breadboard testing and validation for performance was conducted at OVOL's extended range test facility. The facility allows breadboard testing in a controlled environment, where operational environment (absorption and scattering properties) can be accurately and repeatedly generated. In addition to the well-established contrast and resolution technical targets that were used to quantitatively assess whether the UMSLI is 'functional', artificial marine life targets were used during the lab testing phase to generate initial datasets for the classification algorithm development.

Milestone 1.6.1: UMSLI breadboard system testing and quantitative performance validation in controlled turbidity environment

Subtask 1.7: System prototype assembly and integration (M11)

Subtask Summary: Components/subsystems were assembled in field-ready housing modules.

Milestone 1.7.1: UMSLI system modules packaged into underwater housings

Subtask 1.7: System prototype bench-top validation (M12)

Subtask Summary: Field prototype testing of individual image channels and validation of multiplexing algorithms for full omnidirectional functionality in-air was conducted at OVOL.

Milestone 1.7.1: Test readiness review (M12)

Task 2: Prototype Demonstration in a Controlled Environment

Task Summary: This task includes tank testing of the developed UMSLI System and a final test report documenting the completed tank testing was created at the conclusion of this task.

Subtask 2.1: Preparation of test environment at the HBOI Ocean Visibility and Optics Lab (OVOL) facility (M13)

Subtask Summary: The prototype module was installed in the OVOL extended range test tank using existing infrastructure, as well as 2D/3D, moving and stationary targets in the test sequence.

Subtask 2.2: Prototype testing (M14)

Subtask Summary: Prototype testing and validation for in-water performance was conducted at OVOL.

Subtask 2.3: Performance analysis and validation for both coarse and fine modes of operation (M15)

Subtask Summary: System performance of individual illuminators and detectors was evaluated and compared with analytical predictions, using various 2D and 3D technical targets, including a range of artificial marine life targets. Testing progressed incrementally by introducing multiple illuminators to evaluate multiplexing and image sequencing algorithms. Test tank omnidirectional dataset with randomly introduced 3D target objects were produced to assist with the data processing and identification algorithms.

Milestone 2.3.1: Operational Readiness Review (M15)

Task 3: Prototype Demonstration in an Operational Environment (M16-M18)

Task Summary: This task involves the demonstration of the UMSLI prototype in an operating environment along with a report documenting completed testing.

Subtask 3.1: Preparation of field deployment support structure at a coastal site (M16-M18)

Subtask Summary: The field deployment was completed using a midwater mooring, where the infrastructure allows simultaneous monitoring of relevant environmental parameters.

Subtasks 3.2 – 3.3 were completed in Budget Period 2

Task 4: Automated Video Classification (M1-M18)

Task Summary: This task prepared a processing block functionality document which defines interface/interaction with the LiDAR system as well as establishes quantitative performance metrics of the processing framework. Using the Agile Software Development Process, software incorporated research advancements developed in this task: image quality enhancement, Motion History Imaging (MHI), active learning classifier, and active content control. The software was employed to analyze UMSLI scanning LiDAR imagery via automatic classification and archived into a database. A database was developed to store 1) raw LiDAR traces, 2) environment sensor data 3) watermarked intensity image and 4) classification and identification results. The software was integrated with the LiDAR sensor for initial validation testing in the OVOL test tank

Subtask 4.1: Defining overall processing framework (M1-M2)

Subtask Summary: A document was prepared with a detailed description of functions for each processing block and the quantitative metrics that was used to assess the performance of the processing framework. This document defines the interface/interaction between the LiDAR sensing front end and backend processing.

Milestone 4.1.1: Completed processing framework design (M2)

Subtask 4.2: Image enhancement using spatial bilateral pulse shaping (M2-M7)

Subtask Summary: Prior to any processing, LiDAR returns were preprocessed for optimal detection of objects. The spatial-temporal bilateral pulse shaping and deconvolution technique was adapted for this task. The spatial correlation of adjacent LiDAR pulses was exploited via bi-lateral principle, followed by deconvolution using the point spread function predicted by a high-fidelity radiative transfer model: Electro-Optic DEtection Simulator (EODES). Filtering parameters were tuned to adapt to a given system configuration and potential operation environment. Image sequences from the UMSLI technical target testing phase were used to assess the contrast and signal-noise improvement that is possible via this spatial pulse shaping and pre-processing technique.

Milestone 4.2.1: Completion of performance assessment for the UMSLI image quality enhancement technique, through a wide range of test tank conditions.

Subtask 4.3: Developing Motion History Imaging (MHI) based level-one focus of attention detection (M2-M6)

Subtask Summary: Enhanced LiDAR pulses were used to generate a binary MHI. The detection template for 3D MHI signatures were established using training data from the initial UMSLI controlled turbidity tests, and in year 2 augmented with field data. We improved the correlation measure with *correntropy*, a novel measure of similarity that utilizes all even moments of a random variable, and is, therefore, much more accurate than correlation. The detection threshold was first established during the initial field test and optimized during subsequent field tests.

Subtask 4.4: Developing active learning classifier (M2-M12)

Subtask Summary: The high resolution LiDAR image of the background of the monitoring area was built during the initial system deployment period and used as one input to the classifier. To ensure the fidelity of the classifier, scale invariance preprocessing was first performed to segment the image and scale the contour. The pre-defined LiDAR image scanning grid was used to register the background image and the new image containing the penitential object of interest. Once images are registered, they were subtracted, and the presence of moving objects was determined using a Gaussian mean shift algorithm that segments the imagery. Data for clustering is obtained with the pixel-spatial coordinates and intensity. Once the image is segmented, it is normalized for scale.

Milestone 4.4.1: Active learning classifier design readiness review (M12)

Subtask 4.5: Content archiving and retrieval scheme (M3-M9)

Subtask Summary: UMSLI scanning LiDAR imagery was analyzed via automatic classification and archived into a database. Only images with high probability of object of interest were fed into an operator interface. Geo-tag information, time stamp, as well as other relevant environmental variables were embedded into raw imagery using invisible digital watermarking. The database index used to store the current data tuple was embedded into the UMSLI image as invisible watermarking before display and/or storage.

Milestone 4.5.1: Content archiving and retrieval scheme readiness review (M9)

Subtask 4.6: Software integration (M13-M15)

Subtask Summary: The Agile Software Development Process was followed during software development. The majority of Matlab code developed during Subtasks 4.2-4.5 was ported into a Labview™ environment to ensure a seamless interface with LiDAR sensors. For sophisticated algorithms that are difficult to port to Labview, a wrapper was developed so that Matlab functions can be invoked from Labview control. Other Matlab functions with heavier computational overhead were migrated into C to ensure real-time processing capability. A database was developed to store 1) raw LiDAR traces, 2) environment sensor data 3) watermarked intensity image and 4) classification and identification results.

Milestone 4.6.1: Software and database integration review (M15)

Subtask 4.7: Software validation and enhancement using tank data (M15-M18)

Subtask Summary: With the processing software framework in place, the software was integrated with the LiDAR sensor for initial validation test in OVOL test tank. These tests provided an opportunity to identify any deficiency in the algorithms and address them accordingly.

Milestone 4.7.1: Software validated in tank (M18)

Subtasks 4.8 – 4.9 were completed in Budget Period 2.

Task 5: Project Management (M1-M18)

Task Summary: This task is allocated to perform overall and technical project management responsibilities. In addition to overall project oversight, all reporting and data management requirements were managed. Additionally, this task involved consultation with regulatory agencies (NOAA) to assess the longer term potential of the technology. DOE was responsible for coordinating initial discussions with national-level officials.

Subtask 5.1: Resource Agency Overview

Subtask Summary: Worked with DOE to engage cognizant resource agencies to provide information relative to long term project goals of the UMSLI. Intended outcome was to receive responses of the agencies including NOAA, FERC, U.S.Navy, Bureau of Ocean Energy Management, Bureau of Safety and Environmental Enforcement, U.S. Coast Guard, to determine potential system use of the UMSLI system in the marine space.

Milestone 5.1.1: Resource agency meeting conducted (M8)

Go/No-Go Decision Point 1: Hardware and Software Operational (M-18)

Following the controlled environment (test-tank) prototype testing (M14), the detailed information needed for the DOE to make a Go/No-Go decision was provided by the end of month 15. To determine if the project should proceed as initially planned, the demonstrated performance and functionality metrics used to reach a Go/No-Go decision were as follows:

- **Performance:** The system should be capable of obtaining high contrast imagery, with better than 1 centimeter spatial resolution, at a stand-off distance of at least 5 meters in typical clear coastal conditions.
- **Functionality:** The control of pulses, scans and gate timing sequences for the multiple illuminators and receiver subsystems, and correct triggering and multiplexing control at the acquisition electronics should be clearly demonstrated as functional.

As a result of the Go/No-Go decision point, DOE did, at its discretion continued to fund the project.

BUDGET PERIOD 2: M19-M24

Task 3: Prototype Demonstration in an Operational Environment (M19-M20)

Subtask 3.2: Prototype field testing (M19)

Subtask Summary: The field tests were completed in operational environment in the coastal waters in SE Florida. The first series of tests at the mooring site allowed for collection of an omnidirectional dataset over a period of several days with live marine life, artificial marine life targets, and featureless background images to assist with the further development and testing of data processing and identification algorithms. The data was acquired for viewing and quality control purposes using a laptop aboard a support vessel. A secondary means of data collection (e.g., video camera) was used alongside the UMSLI for performance comparison, however due to low ambient light conditions, no useful footage was collected.

Subtask 3.3: Field performance analysis and validation (M20)

Subtask Summary: The second series of tests at the mooring site took place after the processing and detection algorithm was fully developed. During these tests, the algorithm was to be executed with real-time data on the support vessel to allow for instantaneous event detection, automated event-based switching between course and fine scale modes of operation, with live omnidirectional surveillance feed from the UMSLI. System performance and detection results from the field tests were analyzed and compared against analytical predictions and human visual inspection. System performance and functionality was to be validated by assessing the results with functional and operational requirements (i.e., power use, false positive and false negative detections, and classification at various target distances, for various environmental conditions such as light or turbidity).

Milestone 3.3.1: Operational performance results and analysis (M20)

Task 4: Automated Video Classification (M19-M24)

Task Summary: A document was prepared which provides a detailed description of functions of each processing block. This document defined the interface/interaction between the LiDAR sensing front end and backend processing. A design review meeting was to be scheduled upon the completion of this task.

Subtask 4.8: Field test and software hardening (M19-M22)

Subtask Summary: The system was deployed to collect field data for validation, providing content for the database and hardening of the software, algorithm and database.

Milestone 4.8.1: Software and database testing review (M22)

Subtask 4.9: Software and algorithm documentation (M23-M24)

Subtask Summary: The algorithms and software features were summarized in this project's Budget Period 02 Go/No-Go Report. Gnu coding standard was adopted during the software development. The software code, comments and the functionality description were extracted and formatted using the Doxygen tool.

Task 5: Project Management (M19-M24)

Task Summary: This task is allocated to perform overall and technical project management responsibilities. In addition to overall project oversight, all reporting and data management requirements were managed.

3.0 Project Outcomes and Results

As this project's aim was to develop a novel new physical and software system demonstrated in both lab and field conditions, results are presented according to its project phases: 3.1 UMSLI System Design, Specification, and Assembly, 3.2 Prototype Demonstration in Controlled Environment, and 3.3 Prototype Demonstration in Operational Environment.

3.1 UMSLI System Design, Specification, and Assembly

The UMSLI system was prepared with a standard technology development approach: establishing performance metrics, preliminary design, final design, acquisition, and assembly. The outcomes of these phases are described in more detail:

3.1.1 Performance Metric Selection

During Q1 FY15, quantitative performance metrics were evaluated and selected for both optical hardware and classification software. Metrics for the optical system were selected to evaluate image quality: (1) metrics confirmed in test tank conditions – contrast and contrast signal-to-noise ratio, (2) Structure Similarity Index (SSIM), and (3) Z-resolution/temporal noise. Classification software detection metrics included: (1) detection error rate/average false positive rate/average false negative rate, (2) confusion matrix, and (3) receiver operating characteristics (ROC) graphs (ultimately not used in favor of a more intuitive method – False Positive and False Negative Ratios described further in 3.1.3.1.2 Shape Matching-based Classifier). In addition, for classification software content indexing/archiving/retrieving metrics, five metrics were selected: (1) database commits response time, (2) database queries response time, (3) wait statistics, (4) database growth rate, and (5) database throughput. These metrics were submitted as a performance evaluation metrics report and agreed upon by both DOE and FAU.

Portions of a performance metric selection report³ are contained herein to provide background for final project metric selection:

3.1.1.1 Image Quality Metrics

For the Lidar dense scan imaging system front end, image performance was to be characterized using the parameters listed below. These baseline metrics (Contrast and Contrast Signal-to-noise) were to be established through a series of tests in the HBOI test tank. They were then to be optimized prior to field tests.

³ Internal report, submitted to DOE during FY15 Q2 to establish project performance evaluation metrics.

Contrast and Contrast Signal-to-Noise Ratio (CSNR):

$$\text{Contrast: } \frac{\text{WhiteMean} - \text{BlackMean}}{\text{WhiteMean} + \text{BlackMean}}$$

$$\text{Contrast signal-to-noise ratio: } \frac{\text{WhiteMean} - \text{BlackMean}}{\sqrt{\text{WhiteSTD}^2 + \text{BlackSTD}^2}}$$

For a previous project by the team⁴, targets were mounted on a drum which was rotated at a known speed (1 m/s) in order to form a 2D image. A section of the drum with the white-on-black (WoB) technical target is shown in Figure 1. It should be noted that the UMSLI system scans 2D frames, so a moving drum configuration will not be utilized. However, the USAF-52 (US Air Force) target is also of use in establishing the minimum size of feature bar that the imager can resolve. Using such a quantification approach, it should be demonstrable that the system is capable of obtaining high contrast imagery, with better than 1 centimeter spatial resolution, at a stand-off distance of at least 5 meters in typical clear coastal conditions. The system was then expected to be tested in more turbid conditions (identified in Table 1).

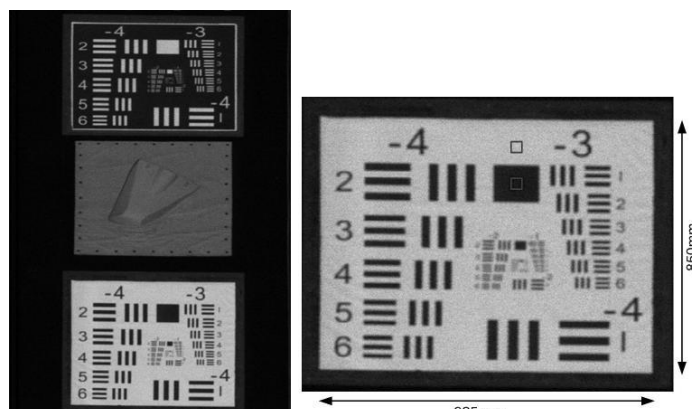


Figure 1 - Left: Laser Line Scan image of entire drum cycle. Right: cropped section of BoW technical target showing target dimensions and image quality analysis regions. The target reflectance was measured in air using a laser and fiber-coupled spectrometer pair

Table 1- Originally proposed and approved UMSLI performance metrics.

Turbidity level	Contrast	Contrast-Signal-Noise-Ratio (raw image)	Smallest Resolvable Bar
Clear water	0.7	15	1cm
> 4 beam attenuation lengths (ALs)	0.2	8	2cm

⁴ Dalgleish, F. R., Caimi, F. M., Britton W. B. and Andren C. F., (2009). 'Improved LLS Imaging Performance in Scattering-dominant Waters,' Proc. of SPIE, Vol. 7317.

Structure Similarity (SSIM) index:

For image quality analysis, a widely adopted image quality metric (SSIM) was expected to be used, which is consistent with human perception⁵.

$$SSIM(I_o, I_r) = \frac{(2\mu_o\mu_r + C_1)(2\sigma_{or} + C_2)}{(\mu_o^2 + \mu_r^2 + C_1)(\sigma_o^2 + \sigma_r^2 + C_2)}$$

An image taken at each target distance under clear water conditions will be adopted as the reference image to evaluate performance at higher turbidities. Table 2 and Figure 2 demonstrated possible imager performance against various test images at different turbidities for the selection of this method. These images consist of both test patterns (Star Chart and Geometry patterns) and images taken in underwater environments (coral, fish, and diver). In Figure 2, an example structural SSIM at various turbidities is shown. As observed in Table 2, quality degrades with increasing turbidity for all of the test images. Attenuation length (AL) used in the table is a unit-less measurement of water turbidity. One AL is the light intensity reduced by 1/e.

Table 2 - Example processed images at different turbidities for a system similar to the UMSLI.

Turbidities	Images					
	Star chart	Geometry	Coral 1	Fish	Coral 2	Diver
Original						
Clear water (0 AL)						
3 AL						
5 AL						
7 AL						

⁵ Z. Wang, A. C. Bovik, H. R. Sheikh and E. P. Simoncelli, "Image quality assessment: From error visibility to structural similarity," IEEE Transactions on Image Processing, vol. 13, no. 4, pp. 600-612, Apr. 2004.

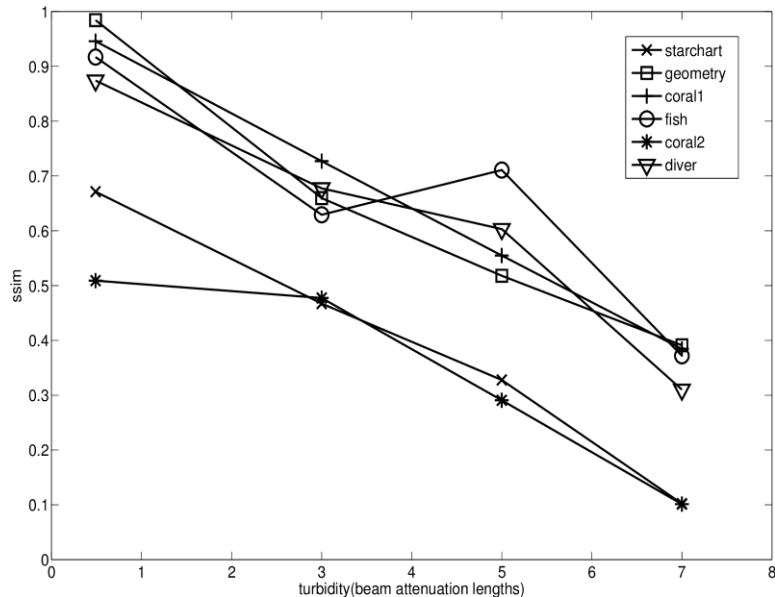


Figure 2 - Example processed image performance at different turbidities (SSIM metrics).

Imaging system speed: During this early stage of development, we assumed that there will be *one region of interest at any given time*. Therefore the imaging system speed was to be evaluated as a function of frequency that objects of interest in the field of view vs. the time required to scan the whole region (i.e., the system will be able to cover the whole region fastest if there is no object of interest and only sparse scan is required, the system speed will decrease with more frequent detection of objects of interest).

3.1.1.2 Detection metrics

The detection algorithm under development was tested against stock fish image datasets to help determine performance for metrics selection. In the Taiwan fish dataset⁶, the algorithm was applied to attempt classify 24 different species of fish. Whereas in the MBARI benthic animal dataset⁷, the algorithm was applied to classify four different species of fish. The initial results are shown in the table below.

Table 3- Preliminary detection algorithm performance with stock fish image data sets.

	Overall error	Aver. false positive	Aver. false negative
Taiwan Sea Fish	2.23±0.59%	18.74±4.72%	0.15±0.04%
MBARI benthic animal	1.08±2.02%	1.50±3.03%	0.35±0.67%

⁶ <http://sourceforge.net/projects/fish4knowledgesourcecode/>

⁷ Edgington D.R., Kerkez I., Cline D.E., Mariette J., Ranzato M., and Perona P., "Detecting Tracking and Classifying Animals in Underwater Video," Proc. IEEE Computer Vision and Pattern Recognition, 2006.

The definition of the overall error rate, average false positive rate and average false negative rate is defined below:

$$FalsePositiveRate = \frac{1}{C_{all}} \sum_{C=1}^{C_{all}} \frac{N_C^C}{N_{\bar{C}}} * 100\%$$

$$FalseNegativeRate = \frac{1}{C_{all}} \sum_{C=1}^{C_{all}} \frac{N_{\bar{C}}^C}{N_C} * 100\%$$

$$OverallError = \frac{\sum_{C=1}^{C_{all}} N_{\bar{C}}^C}{\sum_{C=1}^{C_{all}} N_C} * 100\%$$

Where C_{all} is the total number of classes; N_C , $N_{\bar{C}}$: Number of events that actually belongs to / does not belong to class C ; N_C^C : Number of events that are class C but mislabeled as not C and $N_{\bar{C}}^C$: Number of events that are not class C but mislabeled as C .

Throughout the algorithm development cycle, we intended to fully utilize the radiative transfer model to shorten the development cycle. Therefore, detection metrics were to be categorized through radiative transfer model-based simulations and complemented with test tank experimental dataset when possible.

During this project, to build a solid foundation, we concentrated on classification of coarse granularity (i.e., ability to classify different species – dolphin, turtle or fish). With increased understanding of the dataset and system, we could then investigate improving the classifier to react to finer granularity.

Three dimensional virtual models of the artificial marine life targets suggested by a marine biologist were created for use in algorithm development (example in Figure 3). These 3D models underwent random affine transformations (translation, rotation etc.), and then were run through radiative transfer models with different environment conditions and target distances to generate a dataset. The dataset was to be divided into two subsets – first subset for algorithm development and training and the second subset for testing as well as deriving algorithm performance metrics.

When the imaging system prototype became available for test tank study, we constructed actual 3D targets of the artificial marine species based on the aforementioned 3D models (3.2 Prototype Demonstration in Controlled Environment). Datasets were to be collected for predefined turbidities and target distances used for image quality evaluation. At each turbidity/distance setting, to simulate the object motion, each datum was to consist of the object undergoing two different poses (i.e. predefined rotations and/or translations) using a linear drive.

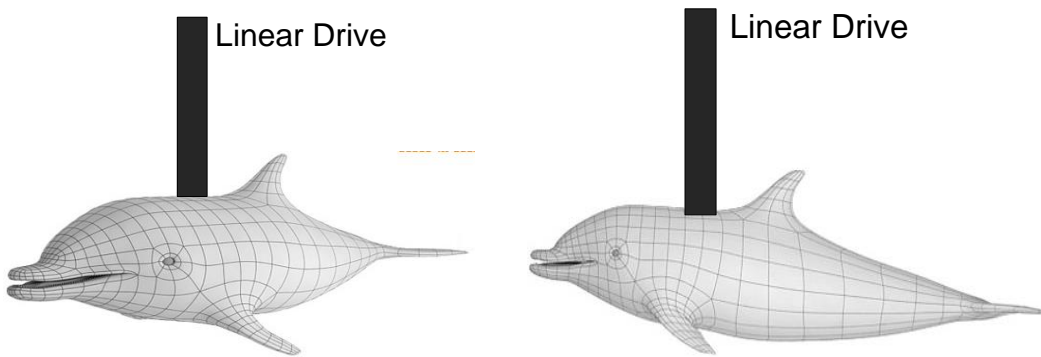


Figure 3 - Illustration of one single datum which consists of the objects at two different poses.

To evaluate the classifier, we retained a more commonly used metric – the confusion matrix⁸. We were to produce a species-specific confusion and the overall success matrices for a series of operation distances and water turbidities. A sample confusion matrix for development of performance metrics is illustrated in Table 4.

Table 4 - Example confusion and performance matrices at different turbidity and target distances.

		Target distance															
		x m					ym										
Turbidity	Clear water	Fish		Dolphin		Turtle		Overall Performance		Fish		Dolphin		Turtle		Overall Performance	
		True Positives	False Positives	True Positives	False Positives	True Positives	False Positives	Species Type	Success Rate	True Positives	False Positives	True Positives	False Positives	True Positives	False Positives	Species Type	Success Rate
		True Positives	False Positives	True Positives	False Positives	True Positives	False Positives	Fish	X%	True Positives	False Positives	True Positives	False Positives	True Positives	False Positives	Fish	X%
Turbidity	C=0.2	False Negatives	True Negatives	False Negatives	True Negatives	False Negatives	True Negatives	Turtle	Y%	False Negatives	True Negatives	False Negatives	True Negatives	False Negatives	True Negatives	Turtle	Y%
		False Negatives	True Negatives	False Negatives	True Negatives	False Negatives	True Negatives	Dolphin	Z%	False Negatives	True Negatives	False Negatives	True Negatives	False Negatives	True Negatives	Dolphin	Z%
		True Positives	False Positives	True Positives	False Positives	True Positives	False Positives	Species Type	Success Rate	True Positives	False Positives	True Positives	False Positives	True Positives	False Positives	Species Type	Success Rate
Turbidity	C=0.2	True Positives	False Positives	True Positives	False Positives	True Positives	False Positives	Fish	X%	True Positives	False Positives	True Positives	False Positives	True Positives	False Positives	Fish	X%
		False Negatives	True Negatives	False Negatives	True Negatives	False Negatives	True Negatives	Turtle	Y%	False Negatives	True Negatives	False Negatives	True Negatives	False Negatives	True Negatives	Turtle	Y%
		False Negatives	True Negatives	False Negatives	True Negatives	False Negatives	True Negatives	Dolphin	Z%	False Negatives	True Negatives	False Negatives	True Negatives	False Negatives	True Negatives	Dolphin	Z%

In order to provide a more intuitive view of the performance of the classifier, we had planned to adopt a receiver operating characteristics (ROC) graphs as well. The common definition of the classifier ROC curve is the true positive (TP) (benefits) vs. false positive (FP) (cost)⁹. However, after receiving feedback from reviewers of submitted manuscripts regarding this approach, we elected to instead use False Positive and False Negative Ratios (3.1.3.1.2 Shape Matching-based Classifier).

⁸ S. V. Stehman. "Selecting and interpreting measures of thematic classification accuracy: Abstract," *Remote Sensing of Environment*: Volume 62, Issue 1, October 1997, Pages 77–89.

⁹ T. Fawcett, "An Introduction to ROC Analysis," *Pattern Recognition Letters*, vol. 27, no. 8, pp. 861-874, 2006.

3.1.1.3 Content indexing, archiving and retrieving metrics

To measure database performance, the following parameters were to be analyzed at a regular interval to ensure the database health:

- Response time for database commits (i.e., database writes);
- Response time for database queries (i.e., database reads);
- Wait statistics (to identify potential I/O bottlenecks);
- Database growth rate;
- Database throughput.

To maintain high database availability, the database was to be backed up at a regular interval and database restore and recovery procedures were to be practiced and documented.

The metric selected to measure the performance of watermarking is the success rate of database index recovery. The main focus was to ensure an operator can interactively interrogate the database for more detailed results from a dataset displayed on an operation interface. It was therefore assumed there would be minimum transformations performed on the dataset. As such, to gather database index recovery success rate, queries were to be conducted using a series of randomized indices. The indices embedded in the data were then to be parsed via watermarking extraction and compared with the actual database indices to determine the success/failure.

3.1.2 Preliminary Design

The Preliminary Design Review (PDR) meeting was held on December 16, 2014. Dr. Fraser Dalglish (Co-Principal Investigator), Dr. Bing Ouyang and Dr. Anni Vuorenkoski provided the technical presentation. Valuable input with regard to the processing framework and the classification metric by Dr. Jose Principe (University of Florida subaward Principal Investigator) was incorporated into the discussion.

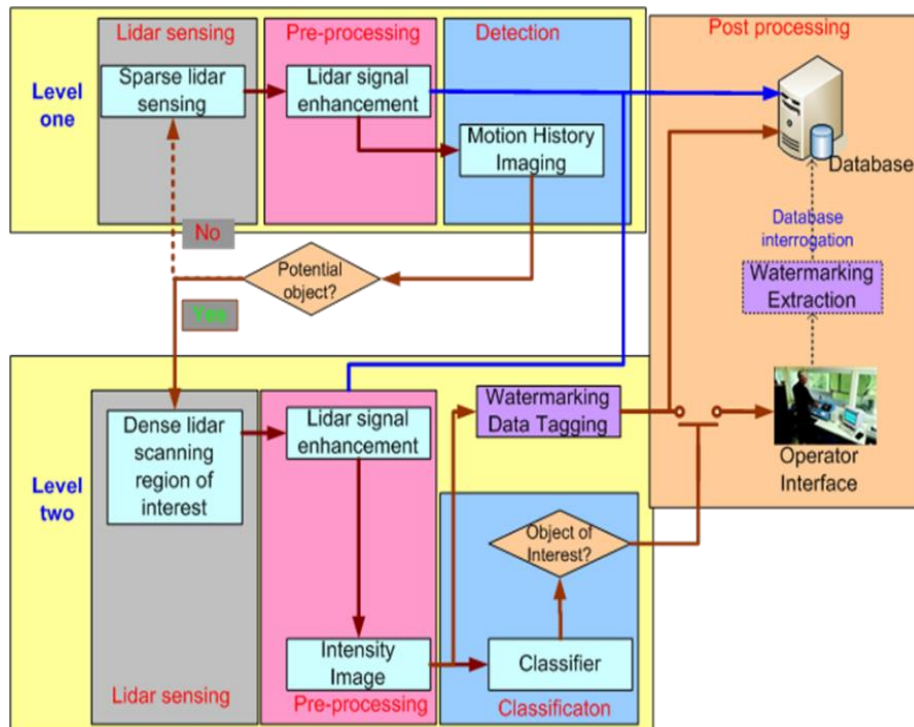


Figure 4 - UMSLI overall processing framework.

The team discussed the System-Level Architecture of UMSLI, with the examination of the proposed Overall Functionality Chart (shown in Figure 4) during the PDR meeting. In this overall system architecture, there was clear emphasis that LiDAR sensor image formation and enhancement functions are closely integrated with detection and classification functions.

The preliminary design of the UMSLI Classification and Post-Processing Software was presented, along with the concepts behind the various aspects being elaborated and discussed in detail: Focus of Attention, LiDAR Signal Enhancement, Object Segmentation, Motion History Imaging, Object Classifier Development, Scale Invariance Processing, and watermarking-based content indexing, archiving and retrieval.

UMSLI Performance Evaluation Metrics were discussed, with consideration given to the appropriate Imaging metrics that were to be used during the test tank and field deployments throughout the stages of system development. The expected contrast and contrast signal to noise (CSNR) values for clear water and more turbid water were discussed, drawing on previous experience with similar imaging LiDAR hardware. Adaptation of the traditional detection and classification metrics to the UMSLI scenario was also discussed in detail.

The UMSLI Hardware/Firmware Design concept was then presented, with detailed examination of optical raytrace results which were conducted as a risk reduction measure to ensure that the MEMS scanners were capable of scanning over a wide angle (up to 100 degrees, which is necessary to keep the number of transmitter/receiver pairs to a minimum for the UMSLI application) whilst maintaining a small beam diameter throughout the volume of interest. The raytrace simulations also included the geometrical and optical attributes of the various candidate components and parts that have been identified for the transmitter assembly.

The need to generate a dataset that consists of multiple images of the various target species (e.g. dolphins, turtles, fish) in different poses and distances from the sensor, through a range of expected turbidities was also emphasized as being critical to the successful development of the active learning classifier.

3.1.3 Final Design

The critical design review meeting was held April 17, 2015 with DOE, project partners, and external observers. No major changes were identified, and the design was approved as presented.

The final UMSLI integrated system adopts a two-tiered design (Figure 4) that consists of the sensing hardware, image understanding (enhancement, detection, classification) and data archiving functional blocks. The UMSLI sensing front end consists of six receivers (Rx, Figure 5 and Figure 6 right), six transmitters (Tx, Figure 5 and Figure 6 left), and a digital signal processor (system diagram in Figure 5). The transmitters artificially “illuminate” a volume of water around an MHK device by scanning a grid of pulses in a bi-directional raster pattern using an analog micromirror device (AMD) and a scan angle expansion lens. As shown in Figure 4, the scan field can be instantly configured to be either sparse or dense, concentrating a lower density pulse grid through a

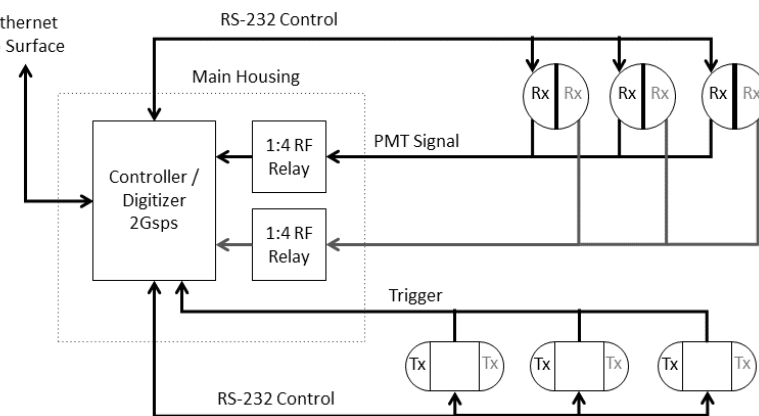


Figure 5 - Final UMSLI system diagram.

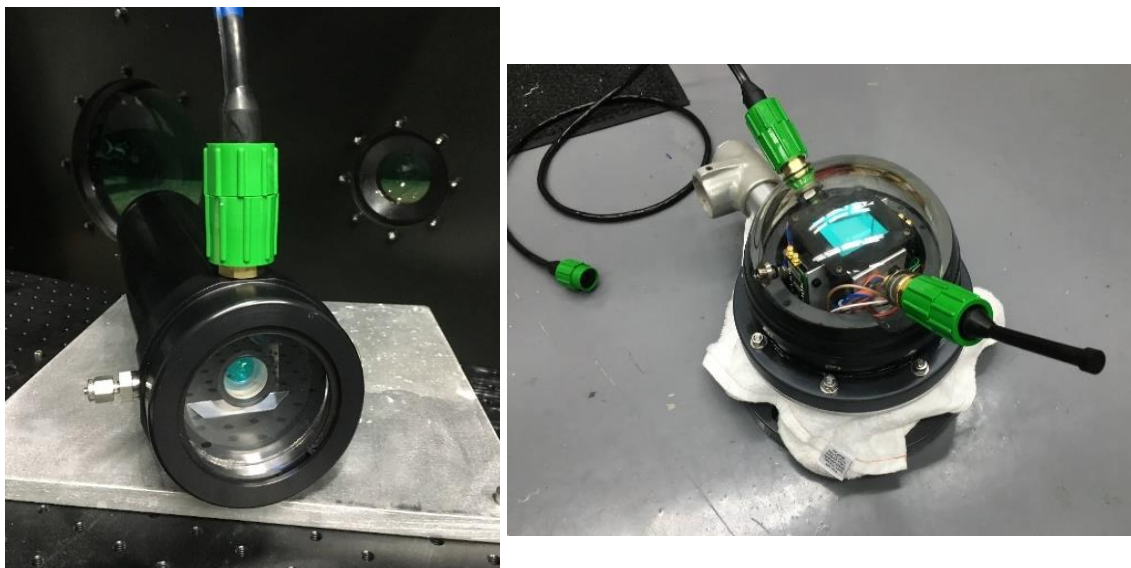


Figure 6 - Fully assembled UMSLI receiver (right) and transmitter (left).

wider range of angles (sparse; level one), or once an object is detected, concentrating a higher pulse density through a narrower range of angles (dense; level two).

The depth of field for each channel of such an imager is governed by the depth of the overlap region between the laser beam and the receiver, while the image resolution is governed by the pulsed laser beam diameter as it intersects a hard target as it traverses between the transmitter and the target. The receivers, which consist of a high-speed photomultiplier module with a focusing optic and spectral bandpass filter, are designed to collect time-resolved returns from the emitted laser pulses, either reflections from objects or scattering in the backward direction.

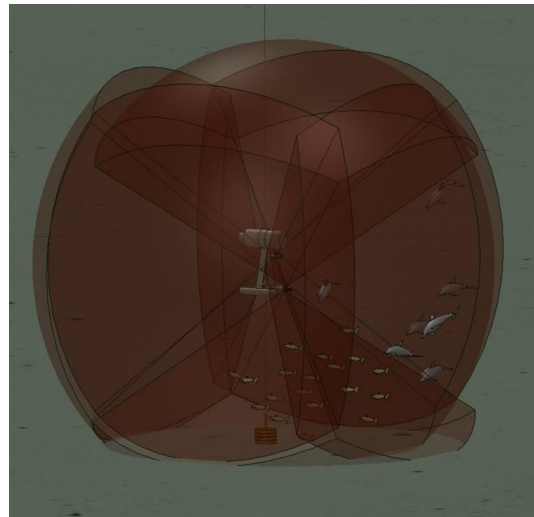


Figure 7 - Rendering showing a constellation of strategically positioned scanned laser transmitters illuminating a complete volume around an MHK device with a greater than 10 meter detection range and 5 meter identification range.

The final image processing system (Pre-processing blocks in Figure 4) includes the following steps:

- a. Gating the waveform to reduce the backscatter and reduce the tail end noise, parameters used: *gating_start* = 40 ns and *tail_end* = 80 ns;
- b. Building a data cube;
- c. Applying a bilateral filter;
- d. Integrating the waveform for each pixel to produce an intensity image;
- e. Applying exponential tone mapping to improve the scene visualization.

3.1.3.1 Classifier Design

The final classifier design, which includes optimizations as a result of controlled environment and field testing, follow. The design is divided into: (1) simulation dataset generation, (2) shape matching-based classifier, and (3) content archiving and retrieval scheme.

3.1.3.1.1 Simulation Dataset Generation

The motivations to create a simulation dataset are:

- 1) To enable the development of the algorithm and the hardware to be conducted in parallel;
- 2) Significantly reduce field test samples.

In essence, the process is to convolve the original image with a point spread function (PSF) determined by the system parameter and water condition and with additional noise corruption:

$$I(x, y) = \mathcal{N}(T(x, y) \otimes PSF(x, y) + n(x, y))$$

The process of generating the simulation dataset (described in Figure 8) is:

- Obtaining 3D models of the objects of interest;
- Creating substantial number of random poses;
- Execute the EODES model to generate data under different environmental conditions and system configuration.

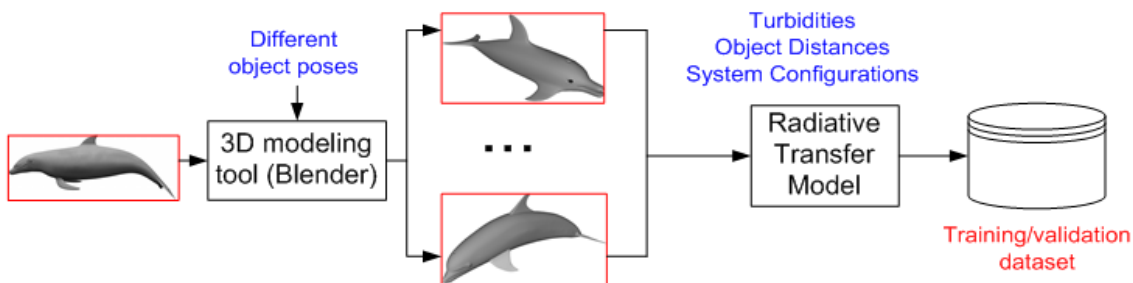


Figure 8 - Process for generating a simulation dataset for the classifier.

3.1.3.1.2 Shape Matching-based Classifier

Here, a shape is characterized by N 2-D points on its contour. The word “shape” is used interchangeably with the point set. A “query shape” Y is the shape whose label is going to be found, whereas a “template shape” X has a known label.

The shape matching-based classifier¹⁰ relies on an enhanced information point set registration to achieve shape recognition. A modified version of shape context (SC) is developed, which is invariant to rigid transformation and flipping¹¹. With the point correspondence obtained by the modified SC, an affine transformation based on the maximum correntropy criterion (MCC) is performed on the query shape. This point set registration could be further refined by non-rigid morphing with the minimization of Cauchy-Schwarz divergence (D_{CS}). Not only does this information theoretical learning (ITL) approach renders excellent registration result, but a new shape similarity measure can also be derived from the registration.

The principle of SC is to describe any point by its relationship with all N points on the same point set. The fundamental difference between SC and point correspondence in aforementioned approaches is that SC is solely based on the property of the shape itself, regardless of a shape's interaction with the other. Major properties of SC include having rich representation ability, being rotational invariant and global. This relationship includes the distance r between two points, and the angle formed by the tangent line at the point and the line connecting the two points. Suppose there are n_r bins for distance and n_θ bins for angles. The cost of matching a point x_i on the query shape X and a point y_j on the template shape Y is

$$C(x_i, y_j) = \sum_{k=1}^{n_r * n_\theta} \frac{[h_i(k) - h_j(k)]^2}{h_i(k) + h_j(k)}$$

where h_i , h_j are the histograms of x_i and y_j . Point correspondences can then be found with the N^*N cost matrix using the Hungarian method. In the implementation, registration is mainly based on information shape matching¹², but with major differences. The affine and non-rigid transformations are performed in consecutive but separate steps, with each step employing a different cost function. By this practice, the transformation spaces are kept separated and calculation of transformation is simplified. Moreover, the probability distribution function (PDF)-based non-rigid transformation can bring variation to SC correspondence based affine transformation. With SC point correspondence available, affine registration becomes a well-defined optimization problem. A common practice to find a reasonable affine transformation A is to minimize the mean squared error (MSE) between XA and the template point set $Y = \{y_i\}_{i=1}^N$, but the presence of outliers (erroneous correspondence) may make MSE suboptimal. Instead, the maximum correntropy criterion (MCC) is picked, which is more robust to outliers:

$$A = \operatorname{argmax} \left(\sum_{i=1}^N G_\sigma(x_i, A, y_i) \right)$$

where $G_\sigma(x_i, A, y_i) = \frac{1}{\sqrt{2\pi\sigma}} \exp\left(-\frac{\|x_i - A y_i\|^2}{2\sigma^2}\right)$. Using the affine transformation as initial condition, a regularized optimization using MCC is adopted to compute the non-rigid transformation. Locality is ensured by small kernel size. The MCC is again adopted for non-rigid transformation. With affine transformation f_{affine} and non-rigid transformation $f_{non-rigid}$, the similarity criterion can be established:

$$\operatorname{corr_cost}_{(X,Y)} = \sum_{i=1}^N G_\sigma(y_i, f_{non-rigid}(f_{affine}(x_i)))$$

¹⁰ Cao, Z., Principe, J., Ouyang, B., Dagleish F., Vuorenkoski A., Ramos B. and Alsenas G., "Marine animal classification using UMSLI in HBOI optical test facility", In *Multimedia Tools and Applications* [In Press];

¹¹ Cao, Z., Principe, J., Ouyang, B.: Information point set registration for shape recognition. In: Proc. ICASSP (2016)

¹² Belongie, S., Malik, J., Puzicha, J.: Shape matching and object recognition using shape contexts. PAMI 24(24), 509–522 (2002)

Figure 9 compares the registration performance of the proposed SC and MCC based shape matching technique against some existing methods. None of the other five registration approaches are as good as the proposed method.

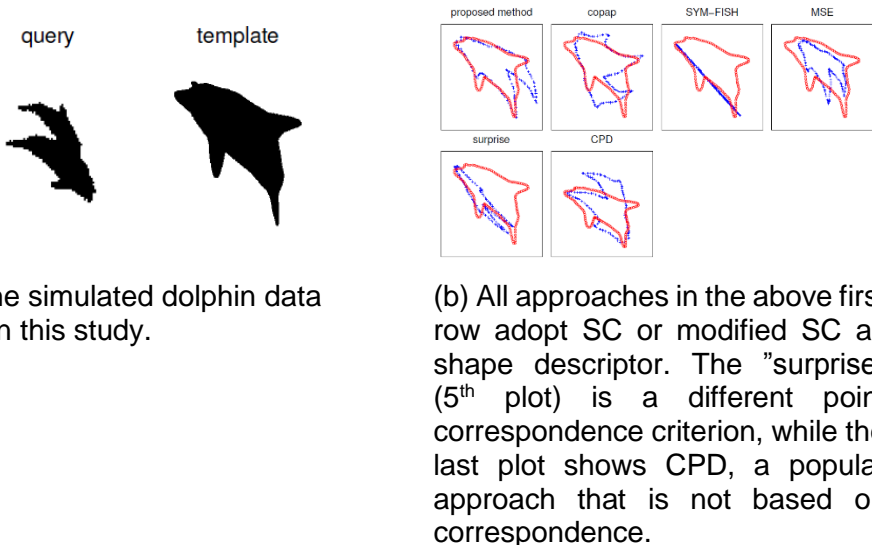


Figure 9 - Comparison of registration performance of proposed SC and MCC-based shape matching technique against some existing methods.

Armed with the robust SC and MCC based point registration, the template matching classification can be described in the following flow chart in Figure 10.

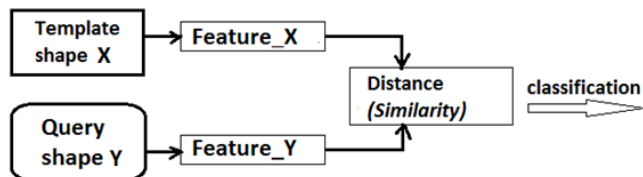


Figure 10 - Template matching classification described in a flow chart.

The classification results using the proposed technique were evaluated using four different similarity measures:

- Method I: SC cost;
- Method II: SC+ instant correntropy cost¹¹;
- Method III: inner distance shape context (IDSC) cost¹³;
- Method IV: IDSC+ dynamic programming (DP) cost¹⁰;

¹³ Liu,W., Pokharel, P.P., Principe, J.C.: Correntropy: properties and applications in non-gaussian signal processing. *IEEE Transactions on Signal Processing* 55(11), 5286–5298

These methods are further illustrated in Figure 11.

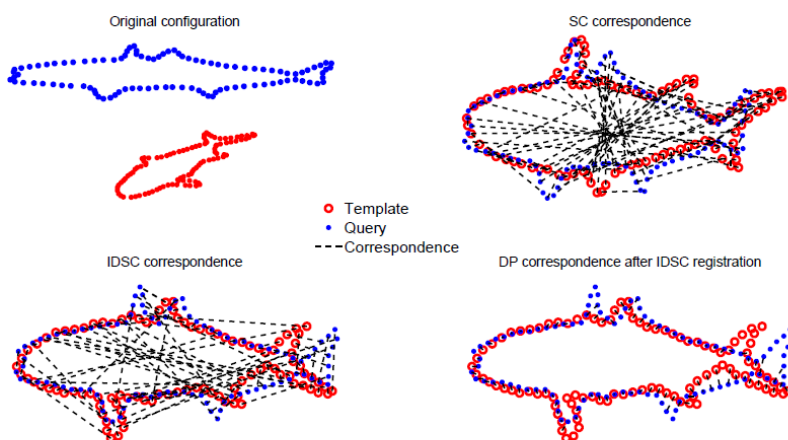


Figure 11 - Illustration of shape registration and similarity cost evaluation. The MCC affine registration results are good for both SC (upper right) and IDSC (lower left) descriptors. Yet neither descriptor actually gives perfect correspondences.

shapes. As many of the templates share a considerable amount of similarity with others, it is desirable to choose a few "representatives" from all 256 templates, which will also significantly reduce computational time in the following classification step. This requires all templates to be represented in the form of vectors, on which a mode-seeking algorithm will be performed. To this end, one can build a 256×256 similarity matrix M using one of the aforementioned methods (e.g. method I). A shape is represented by the corresponding row vector in the similarity matrix after row-wise normalization. The K-means algorithm is then applied to the 256 vectors such that K clusters are found. Within each cluster, the "representative" is simply the vector that has the smallest L1-norm. For $K=10$, the chosen templates are shown in Figure 12.

The clear water query images have in total 8 amberjacks, 6 barracudas and 8 turtles. Three different usages of templates are considered. In the first case, all 256 simulated templates for each species are used. In the second case, one randomly selects 10 templates out of all 256. For this case, 1000 Monte-Carlo trials are conducted and the average accuracy is reported. In the third case, 10 templates are chosen. All 4 methods for measuring similarity are implemented, making 12 combinations in total. For every template usage and every method, a 3×3 confusion matrix is obtained.

This framework has been tested using the test tank dataset acquired at HBOI optical test tank.

The images will first undergo automated segmentation via GrabCut¹⁴. For the more turbid images with $c=0.73$, is set to 1000. GrabCut needs an initialization of background and foreground, which is done by marking the top 25% pixels with largest intensity as foreground.

To generate the template, for each species, a three-dimensional model is generated from a prototype model downloaded from the internet, using the software Blender. The 3-D model is then projected onto different 2-D planes, producing 256 2-D template



Figure 12 - Chosen template shapes. From top to bottom: amberjack, barracuda, and turtle.

¹⁴ Polagye, B., Copping, A., Suryan, R., Kramer, S., Brown-Saracino, J., Smith, C.: Instrumentation for monitoring around marine renewable energy converters: Workshop final report. PNNL-23110 Pacific Northwest National Laboratory, Seattle, Washington (2014)

The classification metrics chosen are therefore:

$$FPR = (\text{total false positives}) / (\text{total false positives} + \text{total true negatives})$$

$$FNR = (\text{total false negatives}) / (\text{total false negatives} + \text{total true positives})$$

Classification result (mean FPR/FNR of the three species) of clear water images is presented in Table 5. Methods I, II, III and IV refer to the similarity measures mentioned above. Effectiveness of any method is best reflected in the last row (average of different template usages). Effectiveness of any template usage is best reflected in the last column. This project did not result in sufficient field data to identify the most promising template, but it is anticipated that additional data will make such a determination possible.

Table 5 - Classification result (mean FPR/FNR of the three species) of clear water images.

Table 6 - Classification result (FPR/FNR) of c=0.73 images.

	I	II	III	IV	Average of I-IV
All 256	0.31/0.64	0.09/0.22	0.13/0.23	0.09/0.15	0.16/0.31
Random 10	0.25/0.49	0.18/0.37	0.17/0.30	0.16/0.26	0.19/0.36
Chosen 10	0.23/0.46	0.16/0.35	0.17/0.28	0.14/0.23	0.18/0.33
Chosen 10 and clear water data	0.16/0.26	0.05/0.08	0.09/0.15	0.09/0.15	0.10/0.16
clear water data	0.16/0.26	0.05/0.08	0.09/0.15	0.07/0.11	0.09/0.15
Average of different template usages	0.22/0.42	0.11/0.22	0.13/0.22	0.11/0.18	\

For c=0.73 (4 attenuation lengths), query images (8 amberjacks, 3 barracudas and 5 turtles), the experiments for clear water images are repeated. In addition, it is critical to examine whether the query shapes generated from clear water images serving as templates can enhance classification accuracy. Therefore, two additional cases are added to the existing three. The first case uses the 10 chosen simulated templates altogether with 8 shapes from clear water images as templates, while only the 8 clear water image shapes are used as templates in the second case. The confusion matrices are shown in Table 6 for all 3 species.

3.1.3.1.3 Content archiving and retrieval scheme

The watermarking-based content archiving and retrieval¹⁵ was also tested using the test tank image. A time stamp was used to embed the index. The watermark embedding process is illustrated in Figure 13. The content retrieval process is illustrated in Figure 14. The time stamp was successfully retrieved from a jpeg encoded image.

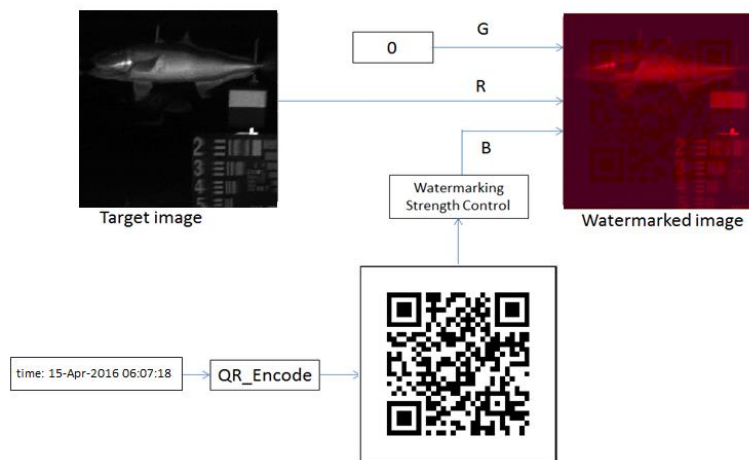


Figure 13 – Watermark embedding process.

The detection/classification (D/C) template library is integrated into the Labview control (LC) module. The LC module controls overall system operations and interacts with the D/C block when new data is available. The LC block will also update the database (DB) with raw LiDAR trace data and other variables (system/environment) and invoking the watermarking module and upload the watermarked intensity image into database. For the database storage, Network Common Data Format (netCDF-4/HDF5) is adopted. Adopting this community-developed standard enables interoperability and helps promote discoverability, interpretation. This provides the foundation for seamless integration with national data centers (i.e., National Data Buoy Center and National Oceanographic Data Center) in the future.

The signal conditioning, detection and classification algorithm have been converted from Matlab code to C++ code. The C++ code has been tested separately on a Linux system (Intel i3 3.4GHz CPU and 8GB memory). For detection, the latency was about 0.04s. For the classifier, the latency was about 3 seconds if 100 templates were used. This is scalable, however, i.e., reducing the time to compute the histogram cost and the Hungarian algorithm and/or reduce the number of templates. Furthermore, the latency for the classifier can be higher than the detection stage since there is no need to provide feedback to the frontend sensor.

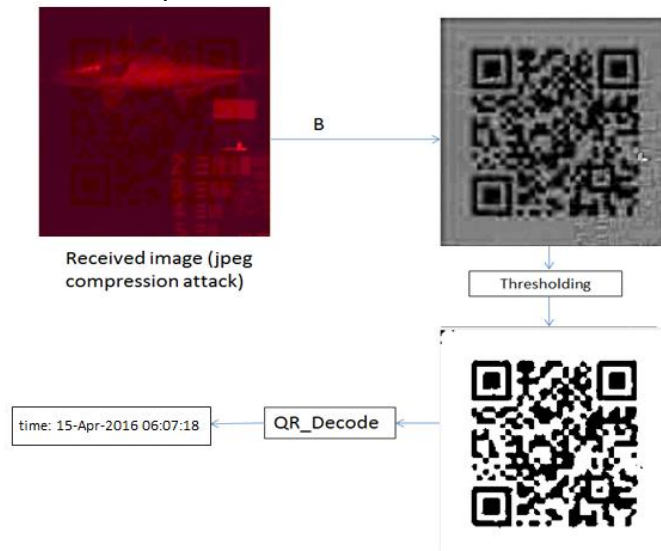


Figure 14 - Content retrieval process.

¹⁵ Ouyang, B.: Watermarking based on unified pattern recognition framework. Ph.D. thesis, Southern Methodist University (2007)

3.2 Prototype Demonstration in Controlled Environment

The goals of this project phase were to: (1) demonstrate system functionality, (2) optimize receiver/transmitter and signal processing performance, and (3) collect preliminary data to further develop and test classification algorithm.

3.2.1 Controlled Testing Environment

The breadboard system was tuned and validated in a laboratory environment (through specially designed optical bulkheads at the FAU Harbor Branch Oceanographic optical testing tank, Figure 15) during Q5. Targets (both technical, Figure 17, and realistic, Figure 16) were used to optimize laser drivers, diodes, scan angles, and lenses in three different turbidity levels. In addition, image processing algorithms began evaluation and tuning.



Figure 15 - FAU HBOI optical testing tank and laboratory.

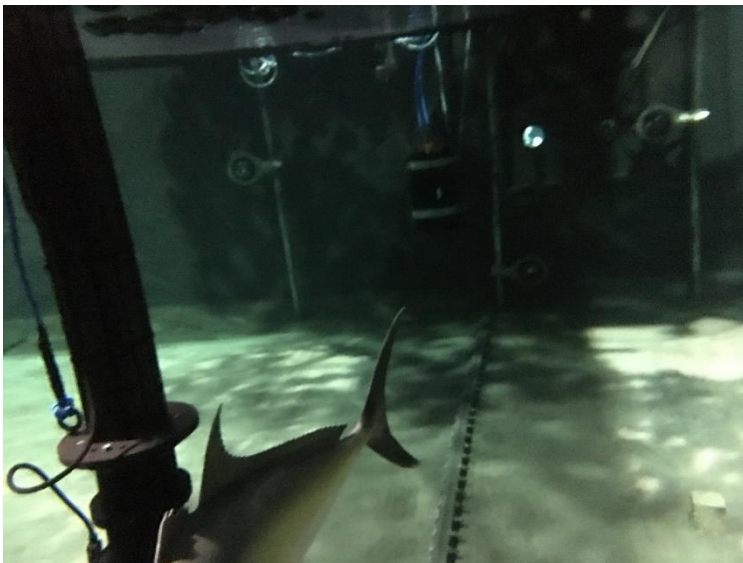


Figure 16 - Artificial realistic aquatic life targets used during controlled environment testing.

3.2.2 System Demonstration and Performance

Several detailed performance metrics were selected for the UMSLI prototype. These include: Contrast Ratio (CR), Contrast Signal-to-Noise Ratio (CSNR), resolvable bar size, Structure Similarity Index (SSI), X-Y Contrast Transfer Function, Z-resolution and temporal noise, and imaging system speed. Results for these metrics are discussed.

3.2.2.1 Image quality metrics

Table 7 summarizes the expected and achieved image quality metric performance.

Table 7 - Image quality metrics performance results and goals.

Turbidity level	CR	CSNR (raw image)	Smallest Resolvable Bar
Clear water GOAL	0.7	15	1cm
Clear water RESULTS	0.8	20	0.25cm
> 4 beam attenuation lengths GOAL	0.2	8	2cm
> 4 beam attenuation lengths RESULTS	0.3	3.23 (processed: 8.5)	1cm

CSNR and CR were computed using the regions marked with yellow dash lines in the image on the right in Figure 17. The USAF target used in the experiment was printed on a 0.5 m x 0.5 m board (left image). The right side, marked with red dash lines, was used to evaluate image resolution. The regions marked with yellow dashed lines were used to evaluate image contrast.

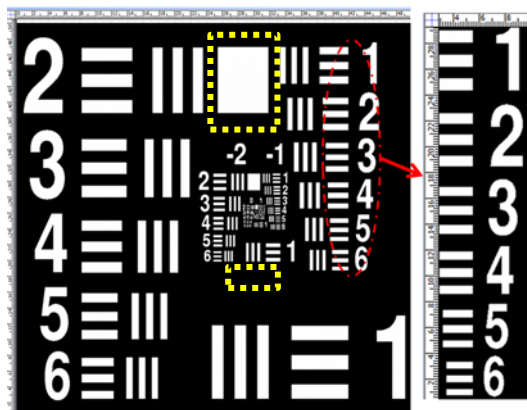
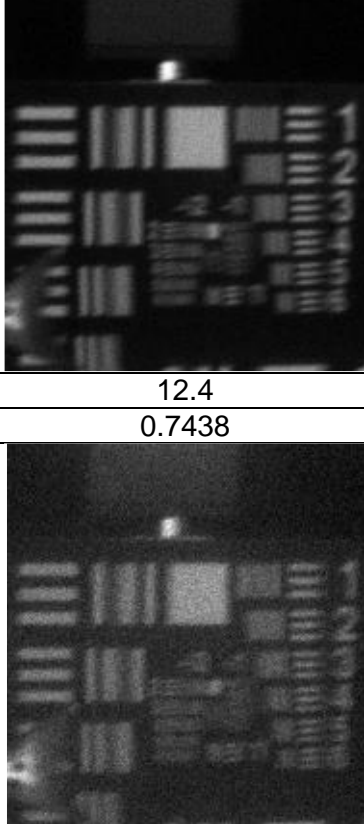
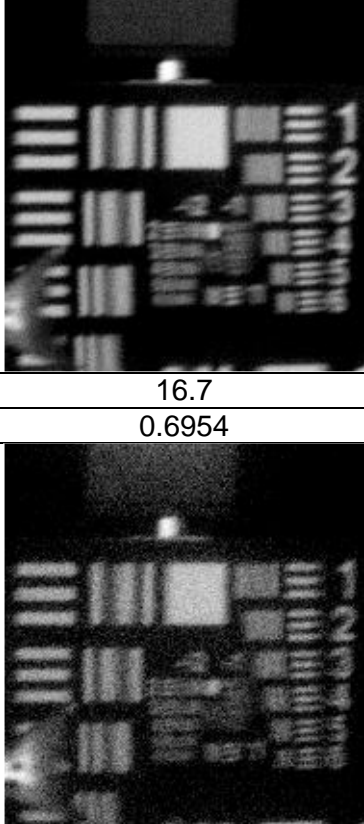
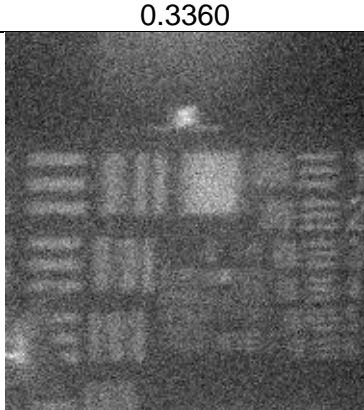
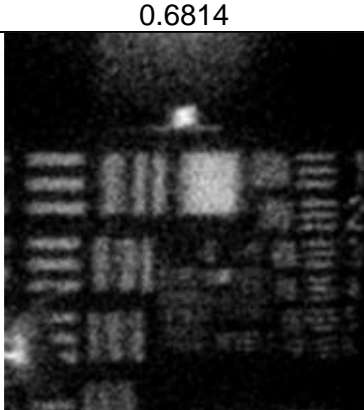


Figure 17 - USAF technical target used to resolve smallest bar and thus resolution.

This resolution target was placed 5.8 m away from the system. Table 8 shows the resolution target at different turbidities. As can be seen from the image, at lower turbidities (clear water), bars next to "6" (spatial resolution of 0.25 cm) are resolvable; at 4.2 attenuation lengths (turbid water), bars next to "1" (spatial resolution of 1 cm) are resolvable. At high turbidities where target signals are more attenuated, periodic noise in the image band is present in the laboratory environment, which degrades the raw image CSNR rating. Field evaluation is expected to remove this interference and improve the system's CSNR raw image performance.

Transmitter settings were chosen because the laser power is the maximum output power obtainable with the current diodes to give us maximum range. Photo Multiplier Tube (PMT) gain settings are a tradeoff between ambient light conditions and distance to an object of interest. High ambient light means the gain must be turned down to not exceed the maximum current from the PMT. Higher gain grants the system longer range. This quantity is adjusted manually, by the user, in real-time.

Table 8 – Controlled Environment testing target resolution at different turbidities.

Turbidity: C=0.4 (2.3 Attenuation Lengths) (transmitter setting: peak power=4.5W, gain=800V)		Original (gated out backscattering)	Processed
	CSNR	20.2	47
	CR	0.8359	0.7581
Turbidity: C=0.53 (3.0 Attenuation Lengths) (power=4.5W, gain=800V)	CSNR	12.4	16.7
	CR	0.7438	0.6954
			
Turbidity: C=0.73 (4.2 Attenuation Lengths) (power=4.5W, gain=800V)	CSNR	3.23	8.58
	CR	0.3360	0.6814
			

3.2.2.2 Detection metrics

Classification results using the proposed techniques were evaluated with different similarity criterion: SC only, correntropy (CORR), SC+CORR and inner distance shape context (IDSC)+dynamic programming (DP).

Table 9 - Classification results using several criterion.

SC only	94.37
Correntropy	97.00
SC+CORR	97.43
IDSC+DP	95.77

During January 28, 2016 test tank experiments, a set of images were taken of an amberjack 3D model in the test tank at a fixed orientation for initial sensor hardware evaluation. Albeit not feasible to obtain meaningful classification statistics with a single data set, the similarity measures of the test tank data at three turbidities against different templates provides insight into classifier performance (Figure 18). Here, the “test tank” curve used a clear water image as the template. For the other three curves, dolphin turtle and fish templates generated with 3D models processed through the EODES model were used. As can be seen below, similarity measure with fish were consistently higher even using the simulated fish as template.

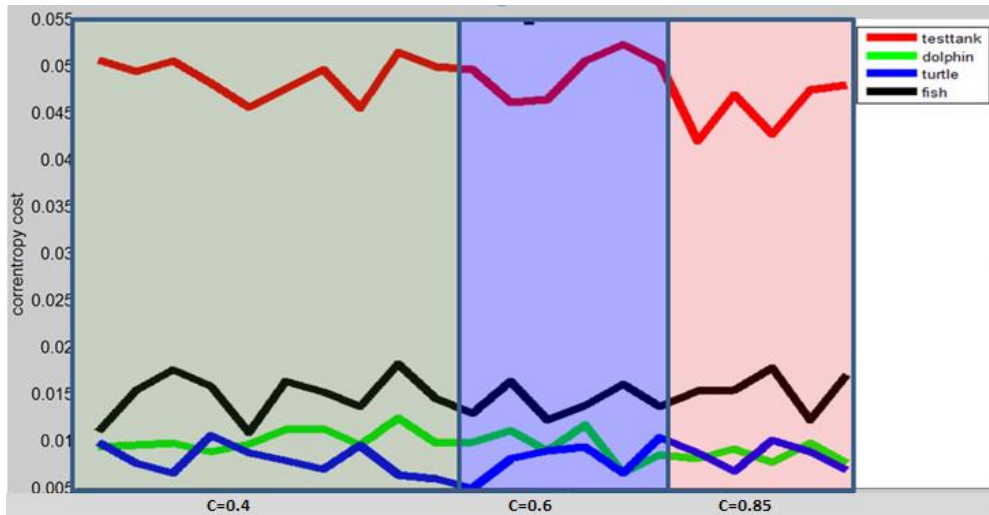


Figure 18 - Similarity measures of test tank data.

Image processing results using test tank are shown in Table 10.

Table 10 - Image processing results with 3D marine life targets during tank testing.

	Original (gated out backscattering)	Processed
Turbidity: C=0.4 Transmitter setting: power=4.5W, gain=800V		
Turbidity: C=0.53 Transmitter setting: power=4.5W, gain=800V		
Turbidity: C=0.73 Transmitter setting: power=4.5W, gain=800V		

3.2.2.3 Software performance metrics

One of the critical requirements of the detection step is to achieve real-time feedback to the sensor front end for subsequent actions. As such, first stage detection involves gating followed by median filtering and level thresholding. On a desktop PC with Intel i3 3.4GHz CPU and 8G memory, the detection was accomplished within 0.04 s (at 25Hz, Figure 19). The implementation comprehends motion history imaging using scans from different time instances, and was tested with the simulated dataset. However, when the target return is sufficient strong, we bypass this last processing step to speed up processing. This is invoked when the ambient interference is high - ambient interference increases with increased water turbidity.

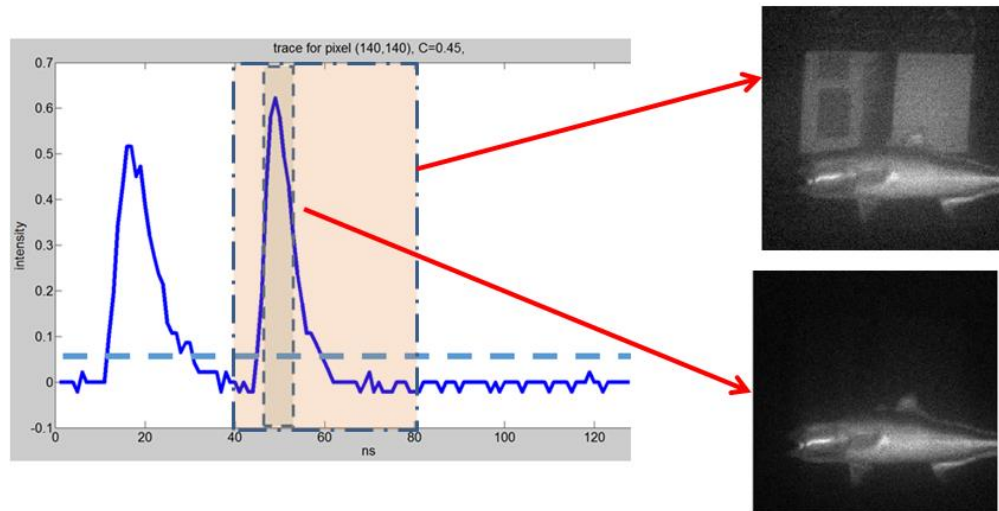


Figure 19 - Detection performance.

3.2.2.4 Functionality

The Tx control board used during laboratory testing controls laser pulse triggering and detector signal timing and acquisition. This board also synchronizes the MEMS scanner with triggering of pulses, a function essential for successful image formation on each channel. The controller in the main electronics housing actuates two 3:1 relays which sequence acquisitions between three orthogonal pairs of bi-directional imaging axes. The control of imaging channels is demonstrated by the results presented for image performance. Experimental data demonstrate an effective embedded software design, as each post-processing block has been tested separately using test tank data.

3.3 Prototype Demonstration in Operational Environment

After successful laboratory evaluation and optimization, the UMSLI system was demonstrated in an operational environment. Short duration (hours) immersion of the system in the coastal waters of Ft. Pierce, Florida allowed the team to evaluate low light, natural turbidity, artificial target, and natural target performance.

3.3.1 Operational Environment Testing Approach

This task was completed during Q2 FY17. Field tests during March 2017 were acquired in turbid coastal ocean conditions near Fort Pierce. Field testing involved attaching receiver housings, transmitter housings, and the digitizer housing to a deployment frame connected via a single electro-mechanical (Ethernet/Power) cable to a moored vessel. The subsea system components were mounted on the deployment frame which has a weight of 220lbs, height of 51.625 inches and width of 37 inches, as shown in Figure 20.

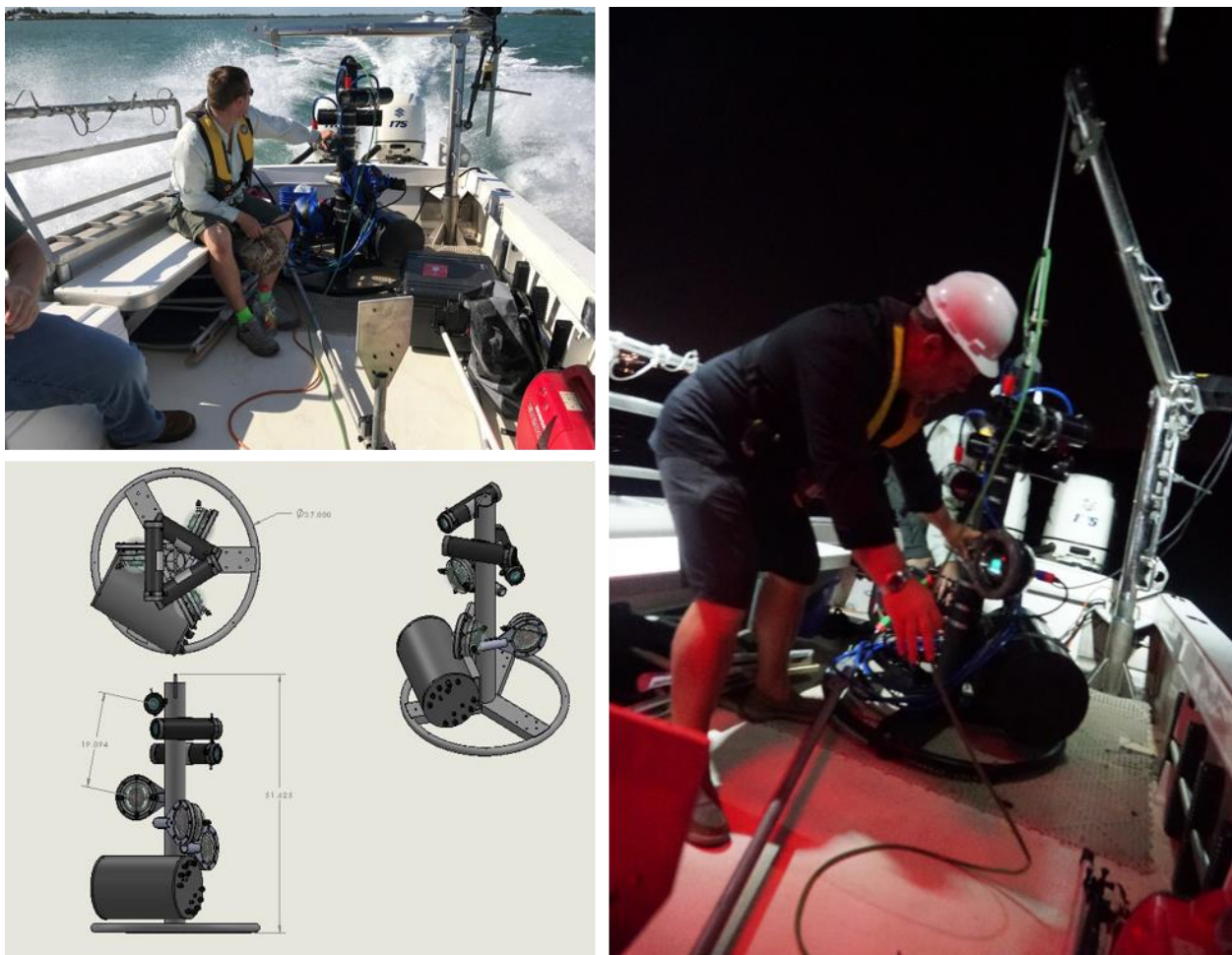


Figure 20 - UMSLI baseline prototype being transported to test site (top left) and deployed (right) in SE Florida during March 2017 field testing. Shown in bottom left are the dimensions (in inches) of the current package.

3.3.2 Results

Field tests were conducted in March 2017 with images of various marine animals targets acquired in coastal ocean conditions near Fort Pierce (FL). During the tests, the beam attenuation coefficient at 638 nm was estimated using the Secchi Depth to be between 0.5 m^{-1} and 1.0 m^{-1} . Interesting results are shown in Figure 21.

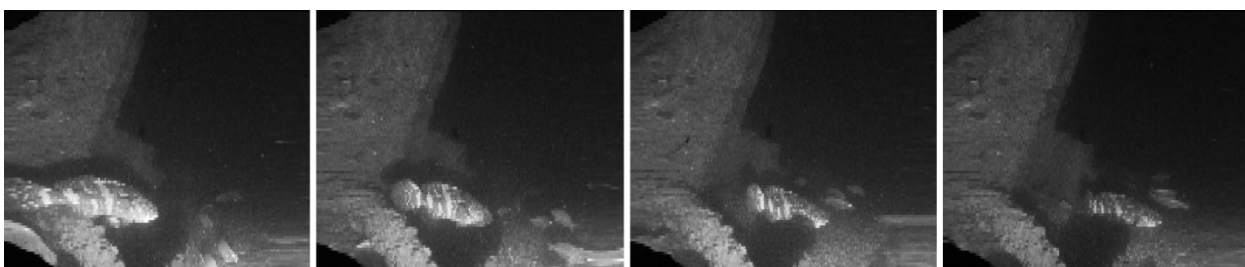


Figure 21 - An image capture sequence taken at 1 frame per second from one of six UMSLI channels.

The images are each acquired using a grid of 200 x 200 pulses, scanned through an angle of 48 degrees by 48 degrees, which is 80% of the maximum transmitter scan angle (coarse scanning mode). Coarse scanning mode is used to determine if objects of interest are within the total field of view. Fine scanning mode is used to identify an object by scanning a bounded box just large enough to contain the object. The 200 x 200 bi-directional raster was completed in 500 ms, using a pulse repetition rate of 80 kHz. The system is operated either manually via a user, or automatically via the two-tiered framework (i.e. detection followed by focus of attention being specified). The system was operated only by the user during project testing. It can transition from coarse to fine scanning mode within a few milliseconds, however. In round-robin scanning mode of three transmitters, after detection from a coarse scan, there is an opportunity for a fine scan of the object in 1 second. A normalized scan area is specified as a percentage of the full scan. Additionally, the number of lines, line speed, resolution and starting position are specified or loaded from a table which is populated by the results of phase I detection and the system computes the required pulse repetition rate.

To allow for both the scan time and the buffering time, the images are taken at 1 frame per second from any two opposite facing UMSLI channels simultaneously, in any sequence. For the images presented in Figure 21, the same channel is being triggered for consecutive captures at 1 frame per second. No post-processing has been performed on the images other than the near-field 40 samples (20 ns or 2.25 m) of backscatter clutter is gated out to reveal a clearer image. The grouper is positioned between 2.25 meters to almost 5 meters from the sensor, with smaller fish visible in the far field.

The images presented in Figure 22 further illustrate the benefit of using digital gating to remove the near-field clutter and other structures around the scene to isolate the fish. The image at the top of Figure 22 generates each pixel by integrating the total samples in the corresponding waveform. A typical waveform at an instant that is reflecting from the body of the Barracuda is shown in the right-hand column, with the blue overlay showing the region of the waveform that the image pixel values are being integrated over. In this image, the Barracuda intersects the beam at a round path time of 110 samples from the moment the pulse is emitted. At 2 Giga samples per second (Gps) digitization rate, this equates to 55 ns. In water light travels 0.225 m in 1 ns, so the total time of flight is 12.375 m. Therefore, the Barracuda is approximately 6.19 m from the sensor.

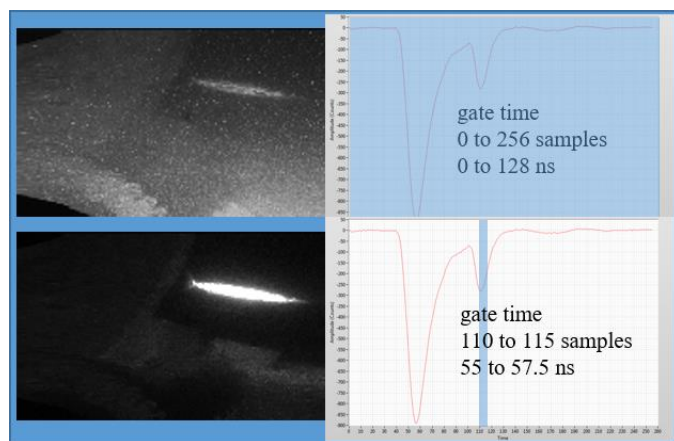


Figure 22 - Raw image captures from field tests of juvenile barracuda. Gate time changes shown on the right.

The 2.5 ns gate timing width produces a range slice width of 0.28 m, which is sufficient to significantly reduce the backscatter clutter and interfering artificial reef structure, therefore increasing the contrast of the Barracuda target to make it a simpler task to automatically extract the fish outline for the classification algorithm.

The images presented in Figure 23 further examine the effect of decreasing the digital gate width to isolate marine animal targets against a complex background scene (one such scene might include moving equipment like a rotating turbine rotor, where if we were to average out multiple frames to remove background and use weighting of frames, we can enhance effectiveness of the current technique).

The case at the top of the figure shows the image constructed from the entire 200 x 200 waveform matrix. This image, which is several reduced in contrast by volumetric scatter is similar to what would be acquired using a continuous wave (cw) laser. The case in the center of the figure shows the wide gate, which is 42.5 ns in duration (or a 4.8 meter slice). This wide gate removes the near-field backscatter, but the artificial reef structures still remain in the image. The case at the bottom of the figure shows the narrow gate, which is 2.5 ns in duration (or a 0.28 meter slice). This narrow gate is effective in removing much of the complex scene structure but still maintains good contrast and resolution for the goliath grouper target.

During field testing, a GoPro high definition camera with a wide angle total view (82 deg x 61.5 deg) was attached to the UMSLI frame. The camera was pointing at a technical target which was placed 2 meters from the camera (Figure 24). During late afternoon conditions, a juvenile goliath grouper was captured swimming in the vicinity of the UMSLI (in the red cropped area shown in Figure 24). Although range is impossible to determine accurately with the camera image, it is estimated that the fish becomes visible at approximately 2.5 meters from the camera (effective field of view of 41 deg x 30.75 deg).

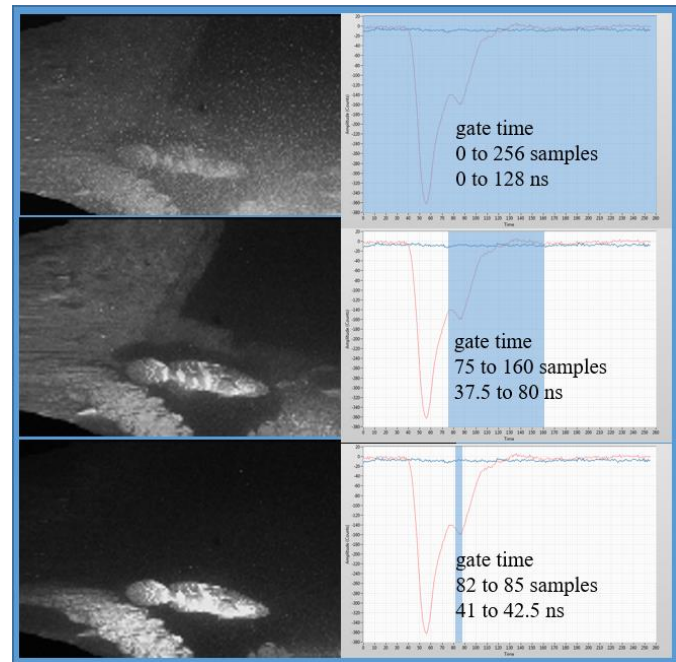


Figure 23 - Raw image captures from field tests of grouper. Gate time changes shown on the right.

During late afternoon conditions, a juvenile goliath grouper was captured swimming in the vicinity of the UMSLI (in the red cropped area shown in Figure 24). Although range is impossible to determine accurately with the camera image, it is estimated that the fish becomes visible at approximately 2.5 meters from the camera (effective field of view of 41 deg x 30.75 deg).

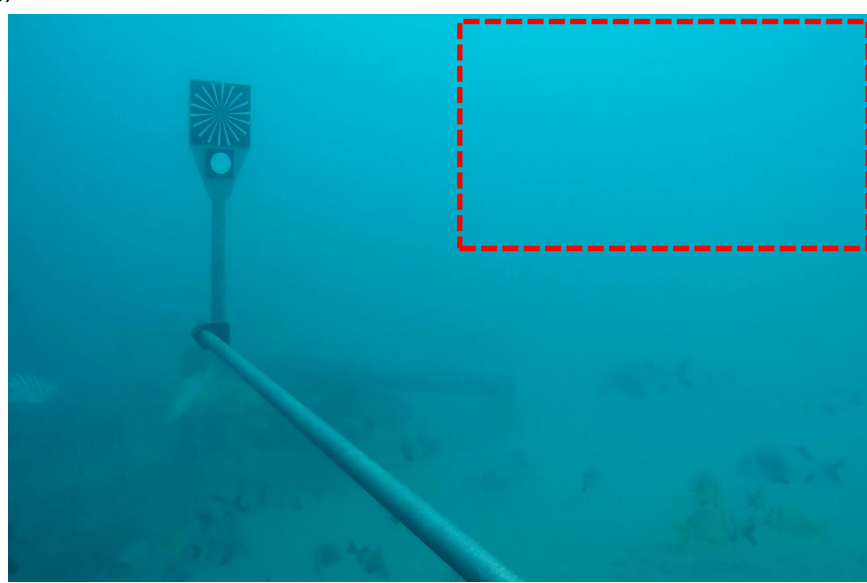


Figure 24 - View from standard high definition camera where grouper was captured.

Figure 26 shows GoPro camera example images from Fort Pierce field tests during March 2017 that demonstrate how it is difficult to identify details on individual fish to determine what species they are. These images were taken in turbid conditions without post processing. The juvenile goliath grouper can be seen moving towards the camera between 2.5 meters and 0.5 meters from the camera (estimated).



Figure 26 - Captured grouper with standard high definition camera.

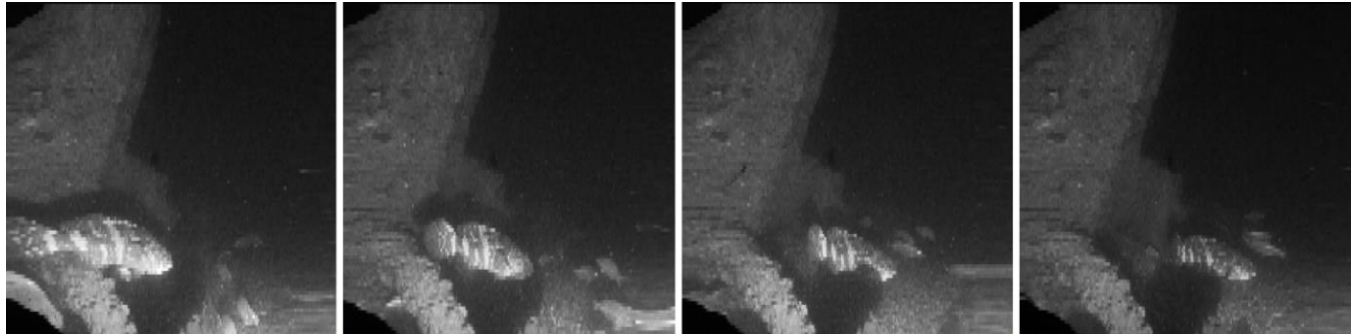


Figure 25 - Captured grouper using UMSLI system.

On the other hand, Figure 25 shows how individual fish can be distinguished using the UMSLI system, at 1 frame per second, from one of six channels. These images were taken in turbid conditions with only near-field 10 ns (1.125 m) backscatter clutter gated out to reveal a clearer image. The juvenile goliath grouper can be seen moving through the foreground around a structure (between 2.2 meters to 5 meters from the sensor), with smaller fish visible in the far field.

4.0 Products/Deliverables

There were several products and deliverables from this project, listed below.

4.1 Publications

Z. Cao, J. C. Principe, B. Ouyang, F. Dalgleish, A. Vuorenkoski, B. Ramos and G. Alsenas, "Marine animal classification using UMSLI in HBOI optical test facility", In *Multimedia Tools and Applications* [In Press].

Z. Cao, S. Yu, B. Ouyang, F. Dalgleish, A. Vuorenkoski, G. Alsenas and J. C. Principe, "Marine Animal Classification with Correntropy Loss Based Multi-view Learning", In *IEEE Journal of Oceanic Engineering* (under review).

4.2 Theses & Dissertations

PhD Dissertation: Z. Cao, "Information Theoretic Classification of Marine Animal using LIDAR Imagery", University of Florida, April, 2017.

4.3 Invited Presentations and Conferences:

F. Dalgleish, B. Ouyang, A. Vuorenkoski, B. Ramos, G. Alsenas, B. Metzger, Z. Cao, J. Principe, "Undersea LiDAR imager for unobtrusive and eye safe marine wildlife detection and classification", In *IEEE/MTS Oceans Europe*, June 2017.

Z. Cao, J. C. Principe and B. Ouyang, Information point set registration for shape recognition, In *ICASSP, IEEE*, Mar. 2016.

Z. Cao, B. Ouyang, F. Dalgleish, A. Vuorenkoski and J. C. Principe, "Marine animal classification using combined CNN and hand-designed image features", In *IEEE/Oceans MTS*, Oct. 2015.

Z. Cao, J. C. Principe and B. Ouyang, "Group feature selection in multiple kernel learning", In *IJCNN, IEEE*, Jul. 2015.

Z. Cao and J. W. Pierre, Electromechanical mode estimation validation using recursive residual whiteness testing, In *North American Power Symposium (NAPS)*, *IEEE*, Sept. 2013.

4.4 Patents:

NA

5.0 Partner Organizations

The following organizations were engaged in this project, in addition to FAU SNMREC and HBOI personnel:

- 1) The University of Florida was included in this project as a subaward. Subaward Principal Investigator Dr. Jose Principe and a PhD graduate student were tasked with classification software development tasks in direct support of this project.
- 2) Battelle Memorial Institute was engaged during proposal stages as a commercialization partner and continued to offer no-cost participation throughout project development. The goal of this engagement was to ensure that prototyping efforts are consistent with technology transfer needs at the conclusion of the project to accelerate commercial availability of this project.

6.0 Recommendations and Conclusions

This project's resulting software and hardware system prototype is useful for demonstrating technological approach feasibility of applying undersea optics to MHK environmental monitoring needs. However, further development is required to transition UMSLI to a commercially viable design. In particular, desirable enhancements include: reducing power consumption for stand-alone deployment, classifier training for a greater variety of species, increasing range of target acquisition in sparse scanning mode, re-packaging for long term fully energetic MHK site deployment, and maximizing the dense scan field of view. UMSLI system performance during high ambient light conditions can be further enhanced with the addition of a condenser lens or a variable attenuator and temporal gating to reduce the loss of dynamic range due to both ambient light collection and the collection of non-image bearing backscattered laser light.

EERE project DE-EE0006787 met its established performance metrics and was demonstrated in both controlled and operational environments. The UMSLI addresses a high priority regulatory requirement to observe marine life interaction near MHK projects. Our solution, translated into a commercial product, will improve resource manager confidence that any harmful interactions between marine animals and marine energy generation equipment are avoided, in a cost-effective and automated solution. Without EERE funding, this novel application of multi-static LiDAR would not have been available to the MHK community for environmental monitoring.